

1 **Title: Causal role for sleep-dependent reactivation of learning-activated sensory**
2 **ensembles for fear memory consolidation**

3
4 Brittany C. Clawson¹, Emily J. Pickup¹, Amy Enseng¹, Laura Geneseo¹, James Shaver¹, John
5 Gonzalez-Amoretti², Meiling Zhao¹, A. Kane York³, Sha Jiang¹, Sara J. Aton^{1#}

6
7 ¹ Department of Molecular, Cellular, and Developmental Biology, University of Michigan, Ann
8 Arbor, MI, USA

9 ² Universidad Ana G. Mendez, Recinto de Gurabo, Gurabo, Puerto Rico

10 ³ Neuroscience Graduate Program, University of Michigan, Ann Arbor, MI, USA

11

12

13

14

15 # Corresponding author:

16 Dr. Sara J. Aton

17 University of Michigan

18 Department of Molecular, Cellular, and Developmental Biology

19 4268 Biological Sciences Building

20 1105 N. University Ave

21 Ann Arbor, MI 48109

22 phone: (734) 615-1576

23 email: saton@umich.edu

24

25

26

27

28 Acknowledgements: The authors are grateful to members of the Aton lab, and to Drs. Natalie
29 Tronson, Monica Dus, Richard Hume, and Dawen Cai for helpful feedback on this manuscript.
30 This work was supported by research grants from the NIH (R01 NS104776) and the Human
31 Frontiers Science Program (N023241-00_RG105) to SJA, a NSF Graduate Research
32 Fellowship to BCC, and a Rackham Graduate Fellowship to BCC.

33

34

35 **Abstract**

36

37 Learning-activated engram neurons play a critical role in memory recall. An untested
38 hypothesis is that these same neurons play an instructive role in offline memory consolidation.
39 Here we show that a visually-cued fear memory is consolidated during post-conditioning sleep
40 in mice. We then use TRAP (targeted recombination in active populations) to genetically label or
41 optogenetically manipulate primary visual cortex (V1) neurons responsive to the visual cue.
42 Following fear conditioning, mice respond to activation of this visual engram population in a
43 manner similar to visual presentation of fear cues. Cue-responsive neurons are selectively
44 reactivated in V1 during post-conditioning sleep. Mimicking visual engram reactivation
45 optogenetically leads to increased representation of the visual cue in V1. Optogenetic inhibition
46 of the engram population during post-conditioning sleep disrupts consolidation of fear memory.
47 We conclude that selective sleep-associated reactivation of learning-activated sensory
48 populations serves as a necessary instructive mechanism for memory consolidation.

49

50 **Introduction**

51

52 Experiences during wake influence neural activity patterns during sleep. For example,
53 hippocampal place cells activated during environmental exploration in wake show higher firing
54 rates (reactivation)¹ and/or similar sequences of activity (replay)²⁻⁶ during subsequent sleep.
55 This phenomenon has been observed in multiple brain regions, multiple species, and following a
56 wide range of experiences⁷⁻¹³. Since sleep loss has a disruptive effect on many forms of
57 memory¹⁴, replay and reactivation may play an instructive role in sleep-dependent memory
58 consolidation^{14,15}. To test this, prior work has disrupted network-wide activity during specific
59 sleep oscillations¹⁶⁻¹⁹ or disruption of activity in genetically-defined cell types across specific
60 phases of sleep²⁰⁻²³- but not the specific neurons activated during learning itself. Recent work
61 has emphasized the essential role of engram neurons in memory recall^{24,25}. To date however,
62 no studies have applied this technology to the question of sleep-dependent memory
63 consolidation.

64

65 Here we test the necessity of sleep-specific engram neuron reactivation for memory
66 consolidation. We describe a form of visually-cued fear memory in mice, which is encoded by
67 single trial conditioning (pairing presentation of an oriented grating visual stimulus with an
68 aversive foot shock) and dependent on post-conditioning sleep. Post-conditioning, the mice
69 behaviorally discriminate between conditioned and neutral visual cues, leading to a selective
70 fear memory. This discrimination is disrupted by post-conditioning sleep deprivation. Using this
71 paradigm, we take advantage of recently developed genetic tools to selectively manipulate
72 orientation-selective (i.e., cue-activated) primary visual cortex (V1) neurons. We find that these
73 cue-activated visual engram neurons are selectively reactivated during sleep in the hours
74 following visually-cued fear conditioning. Optogenetic stimulation of these neurons in awake
75 behaving mice generates a percept of the fear cue, which is sufficient to drive both fear learning
76 and recall. A period of rhythmic optogenetic activation of cue-activated neurons is sufficient to
77 drive functional plasticity - increasing representation of the cue orientation in surrounding V1
78 neurons - and their optogenetic inhibition reduces cue orientation preference. Finally we show
that selective sleep-targeted inhibition of cue-activated V1 neurons during post-conditioning

79 sleep is sufficient to disrupt consolidation of visually-cued fear memory. Based on these
80 findings, we conclude that neurons that are selectively activated in sensory cortical areas during
81 learning play an instructive role in subsequent sleep-dependent memory consolidation.

82

83 **Results**

84

85 **Visually-cued fear memory consolidation is disrupted by sleep deprivation**

86 We first tested the role of sleep in consolidating fear memory associated with a specific
87 visual cue. At ZT0, wild-type mice underwent visually-cued fear conditioning in a novel arena
88 (context A), in which three 30-s presentations of phase-reversing gratings (of a specific
89 orientation X° , shown on 4 LED monitors surrounding the arena) coterminated with a 2-s foot
90 shock. Mice were then returned to their home cage and either allowed *ad lib* sleep for the next
91 12 h, or sleep deprived (SD) for 6 h followed by 6 h of *ad lib* recovery sleep. At ZT12, fear
92 memory for the visual shock cue was assessed in a distinct novel context B. During two
93 separate tests, mice were exposed to gratings of either the same orientation (*i.e.*, shock cue X°)
94 or a different orientation (neutral cue Y°) (**Figure 1a**). As shown in **Figure 1b**, mice allowed *ad*
95 *lib* sleep showed significantly higher freezing responses during presentation of the shock cue
96 than presentation of the neutral cue (two-way RM ANOVA, effect of sleep condition: $p = 0.014$,
97 effect of cue orientation: $p < 0.001$, sleep condition \times orientation interaction: $p = 0.047$). Both
98 sleeping and SD mice discriminated between the shock and neutral cue ($p < 0.0001$ for sleep, p
99 $= 0.03$ for SD, Holm-Sidak *post hoc* test), however, SD mice displayed significantly less freezing
100 to the shock cue than mice allowed *ad lib* sleep ($p = 0.002$, Holm-Sidak *post hoc* test). To
101 compare discrimination between cues, a discrimination index was calculated. Both freely
102 sleeping and SD mice showed discrimination that differed from chance values, however this
103 effect was far clearer in mice allowed *ad lib* sleep (Wilcoxon signed rank test; Sleep: $p = 0.0003$,
104 SD: $p = 0.049$). **Figure 1** shows data for both female and male mice (males - filled symbols,
105 females - open symbols; a breakdown by sex is provided in **Extended Data Figure S1**). Both
106 sexes displayed discrimination between shock and neutral cues when allowed *ad lib* sleep ($p =$
107 0.001 and $p = 0.007$ for males and females respectively, Holm-Sidak *post hoc* test) and
108 impairment when sleep deprived (*N.S.* for shock vs. neutral, Holm-Sidak *post hoc* test). Both
109 sexes showed significant discrimination from random chance only when sleep was allowed ($p =$
110 0.016 for both male and female freely-sleeping mice, *N.S.* for male and female SD mice,
111 Wilcoxon signed rank test). Thus, for subsequent analysis, both sexes were used.

112 The neural circuitry underlying visually-cued fear memory could be altered by sleep.
113 Prior work from our lab has shown that presentation of oriented gratings can initiate response
114 plasticity in neurons of the lateral geniculate nucleus (LGN) and V1, which are consolidated
115 during subsequent sleep^{20,26-28}. However, prior studies of auditory-cued fear have shown
116 conflicting results on the necessity of post-conditioning sleep for consolidation²⁹⁻³². We
117 hypothesized that these discrepancies could be due to differences in timing of either training or
118 testing (or both) between studies. To test this, we performed a time course of fear memory
119 testing for mice conditioned at ZT0. We found that freely-sleeping mice showed differential
120 visual cue discrimination when tested 12, 24, and 36 h after visually-cued fear conditioning -
121 with clear discrimination between shock and neutral cues seen at ZT12 time points (12 and 36 h
122 post-conditioning, $p = 0.001$ and $p < 0.001$ respectively, Holm-Sidak *post hoc* test; **Extended**

123 **Data Figure S2)** but not at ZT0 (24 h post-conditioning; *N.S.*, Holm-Sidak *post hoc* test). At no
124 time point did SD mice discriminate between shock and neutral cues (all *N.S.*, Holm-Sidak *post*
125 *hoc* test). Together these data suggest that visually-cued fear memory consolidation is sleep-
126 dependent, while fear recall may show diurnal rhythmicity.

127

128 **Targeted recombination in activated populations (TRAP) targets orientation-selective,** 129 **fear cue-activated V1 neurons**

130 To characterize and manipulate activity in V1 neuronal populations activated by oriented
131 grating cues (*i.e.*, putative visual engram neurons), we used previously described techniques for
132 TRAP³³. *cfos*-CRE^{ER} mice were crossed to mice expressing tdTomato in a cre-dependent
133 manner (*cfos::tdTom*). The mice were presented with either an oriented grating (X°) or a dark
134 screen stimulus for a 30-min period (**Figure 2a**). Immediately following this presentation, mice
135 were administered tamoxifen and housed in complete darkness for the next 3 days (to prevent
136 additional visually-driven recombination in V1). V1 tdTomato expression (quantified 11 days
137 following tamoxifen administration) was significantly higher in mice exposed to gratings; dark
138 screen presentation induced very low levels of V1 expression (**Figure 2b-c**; nested t-test, $p =$
139 0.0001).

140 To test the orientation selectivity of X°-activated TRAPed neurons, mice were presented
141 with either the same oriented grating (X°) or an alternate oriented grating (Y°) prior to sacrifice
142 (**Figure 2d**). TRAPed V1 neurons show a significantly higher percent cFos expression following
143 re-exposure to the same orientation than following exposure to a different orientation (X°- $32 \pm$
144 3% vs. Y°- $21 \pm 2\%$; $p = 0.009$, nested t-test; **Figure 2e-f**). This level and specificity of cFos
145 overlap is comparable to that reported for auditory stimuli in cochlear nuclei (Guenther et al
146 2013). Together these data suggest that TRAP provides genetic access to orientation-selective
147 V1 neurons activated by oriented grating stimuli.

148

149 **Optogenetic activation of TRAPed V1 neurons generates a orientation-specific percept**

150 To further test the cue selectivity of recombination in neurons activated by an oriented
151 grating (X°), and to test the behavioral significance of activity in this neuronal population, we
152 expressed ChR2 in X°-activated TRAPed neurons (*cfos::ChR2*). As shown in **Figure 3a**,
153 *cfos::ChR2* mice implanted with bilateral V1 optic fibers were presented with a single oriented
154 grating (X°) for TRAP as described above; 11 days later, one of two variants of the visually-cued
155 fear conditioning were performed. The first subset of mice were conditioned at ZT0 using
156 rhythmic (1Hz) optogenetic activation of TRAPed V1 neurons (rather than oriented grating
157 presentation) as a cue for foot shock (**Figure 3b**). Mice were returned to their home cages,
158 allowed *ad lib* sleep, and tested at ZT12 in a dissimilar context. At this point, mice were
159 presented with oriented gratings of the same orientation used for TRAP (X°) and a different (Y°)
160 orientation. Presentation of X° elicited significantly greater freezing responses than presentation
161 of Y° (ratio paired t-test, $p = 0.008$; Wilcoxon signed rank test vs. chance, $p = 0.02$) (**Figure 3c**).

162 In a second set of experiments (**Figure 3d**), mice underwent visually-cued fear
163 conditioning at ZT0, using X° gratings as the shock cue. At ZT12, they were placed in a
164 dissimilar context, where after a delay they received bilateral 1 Hz optogenetic stimulation of
165 TRAPed V1 neurons. These mice showed significantly greater freezing behavior during
166 optogenetic stimulation than before and after stimulation (**Figure 3e**; $p = 0.003$ for each Holm-

167 Sidak *post hoc* test). Both of these results indicate that optogenetic activation of the X°-activated
168 TRAPed V1 ensemble is sufficient to generate a percept of the X° visual cue, consistent with
169 recent data³⁴. Moreover, these data demonstrate that optogenetically-activated V1 neurons can
170 substitute behaviorally as a visual cue for either encoding or recalling fear memory. Together,
171 this suggests that activity of the X°-activated TRAPed ensemble in V1 constitutes an engram for
172 the visual cue.

173

174 **Orientation-selective V1 ensembles are reactivated during post cued fear conditioning** 175 **sleep**

176 Since sleep facilitates consolidation of visually-cued fear memory, and the TRAPed
177 ensemble provides cue-selective information, we next evaluated whether the TRAPed
178 population is selectively activated during post-conditioning sleep. We again expressed tdTomato
179 in TRAPed X°-activated neurons (*cfos::tdTom*). As shown in **Figure 4a**, these mice were
180 presented with X° to induce tdTomato expression, and 11 d later were cue conditioned using
181 either the same X° oriented grating stimulus, or a dissimilar Y° stimulus. They were then
182 returned to their home cage and allowed *ad lib* sleep over the next 4.5 h, at which point they
183 were sacrificed for V1 cFos immunostaining. When X° was used as the fear conditioning cue, 34
184 $\pm 2\%$ of tdTomato-expressing V1 neurons showed expression of cFos after subsequent sleep
185 (**Figure 4b**) - a level similar to that seen after same-orientation grating exposure (**Figure 2e**).
186 When mice were instead conditioned using Y° as the shock cue, the percent overlap was
187 significantly lower ($26 \pm 1\%$). These data suggest V1 neurons activated by a visually-cued
188 learning experience are more likely to remain active during post-learning sleep, consistent with
189 observations of ensemble reactivation in V1 following other types of learning⁷. Thus sleep-
190 associated V1 ensemble reactivation could serve as a plausible substrate underlying visually-
191 cued fear memory consolidation.

192

193 **Rhythmic offline reactivation of orientation-selective V1 ensembles induces plasticity** 194 **and alters representation of orientation in V1**

195 To test whether sleep-associated reactivation of orientation-selective neurons could
196 impact the representation of orientation across V1, we tested how rhythmic optogenetic
197 activation of X°-activated TRAPed neurons affected surrounding V1 neurons' response
198 properties. We recorded neuronal firing patterns and visual responses in V1 from anesthetized
199 *cfos::ChR2* mice before, during and after a period of rhythmic (1 Hz) light delivery. We first
200 generated tuning curves to assess orientation preference for each V1 neuron, measuring firing
201 rate responses to a series of 8 different oriented gratings. This orientation preference test was
202 followed by a 20-30 min period without optogenetic stimulation, a second orientation preference
203 test, a 20-30 min period of 1 Hz optogenetic stimulation, and then a final orientation preference
204 assessment (**Figure 5a**).

205 V1 neurons showed heterogeneous firing responses during rhythmic optogenetic
206 stimulation (**Figure 5b**). A small fraction of the recorded neurons (4%) were activated
207 immediately following initiation of the 10-ms light pulses, 1% were significantly inhibited, and 1%
208 showed only long-latency (more than 200 ms) excitatory responses. The remaining recorded
209 neurons were either unaffected by optogenetic stimulation (44%) or showed consistent
210 activation 14-50 ms after light pulses (49%), suggesting these neurons receive excitatory input

211 from the optogenetically-stimulated population (**Figure 5c**). Rhythmic activation of the X°-
212 activated V1 population did not significantly alter the V1 local field potential (LFP) power
213 spectrum (**Figure 5d**, *N.S.*, K-S test).

214 To assess how optogenetic reactivation of the X°-activated TRAPed population affects
215 response properties in surrounding V1 neurons, orientation tuning curves for well-isolated and
216 stably-recorded neurons were compared before vs. after optogenetic stimulation. While
217 orientation preference for X° (vs. X+90°) was stable across 20-30 min period without
218 optogenetic stimulation, a similar period of 1 Hz light delivery caused a selective shift in
219 orientation preference across V1 toward the orientation of the TRAPed population. Shifts in
220 orientation preference towards the orientation of the TRAPed ensemble (X°) were greater for
221 those neurons that showed consistent excitatory responses 20-50 ms following light pulses,
222 relative to neurons that did not show these responses (*N.S.* for non-activated neurons, vs. $p =$
223 0.002 for activated neurons, nested t-test; **Figure 5e,f**). Critically, this shift is similar to that seen
224 in V1 after presentation of oriented gratings, followed by a subsequent period of *ad lib*
225 sleep^{20,27,28}.

226

227 **Sleep-associated reactivation of orientation-selective V1 neurons is necessary for** 228 **consolidation of visually-cued fear memory**

229 Because reactivation of orientation-selective V1 populations occurs during post-visually-
230 cued conditioning sleep, and is sufficient to induce changes in orientation representations in V1,
231 we next tested the necessity of sleep-associated ensemble reactivation for consolidation of
232 visually-cued fear memory. To assess how inhibition of the X°-activated TRAPed population
233 affects firing in surrounding V1 neurons, we expressed ArchT in *cfos*-CRE^{ER} mice (*cfos::Arch*).
234 We recorded spontaneous activity and visual responses in V1 neurons in anesthetized mice
235 before and during a period of optogenetic inhibition (**Figure 6a**). Periodic inhibition (cycles of 5 s
236 light delivery, followed by a 0.5 s ramp off, and 1 s off) led to heterogeneous changes in
237 spontaneous firing (**Figure 6b-c**), with 34% showing no response (\pm 0-5% change in firing rate),
238 21% activated (> 5% increase in firing rate) and 34%, 9%, and 2%, respectively, inhibited
239 slightly (6-33% decrease in firing rate), moderately (34-66% decrease), or strongly (67-100%
240 decrease). Inhibition did not affect V1 LFP power spectra (**Figure 6d**, *N.S.*, K-S test). Inhibition
241 during presentation of oriented gratings led to a significant decrease in orientation preference
242 for X° in inhibited neurons (**Figure 6f**, $p = 0.007$, nested t-test). There was no significant shift in
243 non-inhibited neurons (**Figure 6e**, *N.S.*, nested t-test). Together, these data indicate that
244 inhibition of the TRAPed ensemble leads to changes in orientation representation across the
245 population, without grossly disrupting network activity across V1.

246 We next asked whether sleep-targeted inhibition of V1 visual engram neurons (i.e.,
247 those encoding the fear memory cues) disrupts consolidation of visually-cued fear memory. For
248 these experiments, *cfos::Arch* mice expressing ArchT in X°-activated neurons (and control mice
249 not expressing ArchT) underwent visually-cued fear conditioning in context A at ZT0, using
250 either X° or Y° as a cue for foot shock (**Figure 7a**). They were then returned to their home
251 cages for *ad lib* sleep. For the first 6 h following conditioning (a window of time where SD
252 disrupts consolidation; **Figure 1**), TRAPed neurons in V1 were optogenetically inhibited (using
253 the parameters described for **Figure 6** above) during bouts of NREM and REM sleep
254 (**Extended Data Figure S3**). This pattern of inhibition did not significantly alter either sleep

255 architecture or V1 EEG power spectra (which were similar between inhibited and control mice;
256 **Extended Data Figure S4**).

257 At ZT12, mice were presented with X° and Y° oriented gratings (shock and neutral
258 cues) in a dissimilar context B. In mice presented with X° as a cue for foot shock, sleep-targeted
259 optogenetic inhibition of TRAPed V1 neurons prevented fear discrimination between X° and Y°
260 cues during testing. These mice showed high levels of generalized fear (i.e., high levels of
261 freezing in response to presentation both gratings) - indicating disrupted fear memory
262 consolidation. In contrast, both control mice (not expressing ArchT) and mice presented with Y°
263 as the shock cue showed cued fear memory consolidation and discriminated between shock
264 and neutral cues at ZT12 (**Figure 7b-c**). Together these data suggest that selective reactivation
265 of V1 visual engram neurons during post-learning sleep provides an essential substrate for
266 consolidation of an associative visually-cued memory.

267

268 **Discussion**

269 Our present data demonstrate that orientation-selective V1 neurons involved in encoding
270 a specific visually-cued fear memory (visual engram neurons) play an ongoing role in memory
271 consolidation during subsequent sleep. After selective activation of these neurons during
272 visually-cued fear conditioning, these neurons continue to be active during sleep in the
273 subsequent hours (**Figure 4**) - a time window during which sleep plays a role in promoting
274 consolidation (**Figure 1**). Activity in these neurons is sufficient to drive a percept which can
275 substitute for the visual fear cue in mice during wake (**Figure 3**). It remains unclear how
276 selective sleep-associated reactivation of these neurons affects the surrounding visual cortex
277 (or interacts with circuitry engaged selectively by aversive conditioning). However, periodic
278 optogenetic activation of these orientation-selective neurons is sufficient to drive shifts in
279 orientation preference in surrounding neurons that show excitatory postsynaptic responses to
280 their input (**Figure 5**). This leads to an increase in the representation of the visual engram
281 neurons' preferred orientation in the surrounding V1 network. While the functions of such an
282 increase in representation are currently unknown, this increase in representation for a specific
283 orientation is seen in the visual cortex in mice^{20,27,28,35,36}, human subjects^{37,38}, and nonhuman
284 primates^{39,40} as a result of orientation-specific experience and task training. Thus changes in
285 representation in sensory cortex appear to be either a correlate, or a cause, of changes in
286 orientation discrimination ability with experience.

287 We show conversely, that optogenetic inhibition of orientation-selective neurons acutely
288 reduces the representation for the visual engram neurons' preferred orientation in the
289 surrounding V1 network (**Figure 6**). Finally, we demonstrate that optogenetic inhibition of these
290 visual engram neurons during post-conditioning sleep dramatically disrupts consolidation of fear
291 memories for specific visual cues (**Figure 7**). Mice with sleep-targeted inhibition of cue-activated
292 neurons show high levels of general freezing behavior at testing, but no discrimination between
293 cues of different orientations. Thus their specific memory deficit seems to be due to an inability
294 to link fear memory to a specific orientation cue during consolidation, rather than a disruption of
295 fear memory *per se*.

296 This work links together two bodies of literature regarding the neural substrates of
297 memory. One recent area of investigation has focused on the role of engram neurons which are
298 activated by learning experiences, and whose activation is necessary and sufficient for memory

299 recall^{24,25,41}. However, the role these neurons play in the consolidation of memories following
300 learning has been a matter of speculation. Here we show that the neurons engaged during
301 learning play a necessary and instructive role during subsequent sleep. The second body of
302 literature has focused on replay of learning-associated activity patterns in specific neuronal
303 ensembles as a mechanism for sleep-dependent facilitation of memory storage. While the
304 phenomenon of replay during sleep has been widely reported^{2,7,21,22,42}, a causal role for sleep-
305 dependent replay in memory consolidation has been difficult to prove. At least two technical
306 obstacles have slowed progress toward understanding the role of replay in sleep-dependent
307 consolidation. First, many tasks used in rodents to study phenomena (e.g. maze running) that
308 require several days of training prior to obtaining recordings of sequential firing patterns - a
309 timescale incompatible with memory consolidation occurring across a single sleep period.
310 Second, many prior studies aimed at addressing the question of replay's necessity for
311 consolidation have relied on disrupting circuit-level activity across windows of sleep^{18,19},
312 sometimes over several days^{16,17}. Here we have taken advantage of recently-developed genetic
313 tools to label cue-activated neurons³³ and a new single trial paradigm for studying sleep-
314 dependent consolidation of memory for a specific sensory cue (**Figure 1**). These have allowed
315 us to demonstrate that sleep-associated reactivation of cue-activated visual engram neurons
316 plays a critical, instructive role in consolidating an associative memory linked to that cue.

317 A limitation of the present study is that inhibition of visual engram neurons in V1
318 occurred throughout all stages of sleep (i.e., both REM and NREM). Our prior work on
319 experience-dependent plasticity in V1 has demonstrated that thalamocortical oscillations
320 coordinating activity between the lateral geniculate nucleus (LGN) and V1 during NREM sleep
321 are essential for orientation preference shifts in V1²⁰. The pattern of optogenetic stimulation
322 used on visual cue-activated neurons in this study (i.e., regular periodic activation at 1 Hz) is in
323 some ways similar to what occurs in V1 during these NREM oscillations. Critically, this pattern
324 of activation is sufficient to drive large V1 orientation preference shifts (**Figure 5**). However, a
325 role for REM activity in cortical plasticity cannot be ruled out. REM plays a critical role in
326 developmentally-regulated experience-dependent plasticity in V1⁴³. In many species, REM is
327 characterized by selective activation of LGN-V1 circuitry during pontine-geniculate-occipital
328 (PGO) waves, which promote synaptic plasticity in various brain structures¹⁴. Future work will be
329 aimed at both characterizing patterns of activity in orientation-selective populations during REM
330 vs. NREM, and in targeting inhibition of this population to specific states.

331 The present findings may ultimately inform our understanding of how sensory cortical
332 areas interact with structures such as the hippocampus and amygdala during sleep, and how
333 these interactions inform consolidation of specific memories. Together our data indicate that
334 primary sensory structures engaged in fear memory encoding communicate with structures
335 conveying emotional valence information during post-learning sleep to promote long-lasting fear
336 association with a specific cue. Whether this interregional communication is unique to one or
337 more sleep states is a critical unanswered question. Answering this question may have
338 important implications not only for understanding sleep's mechanistic role in memory
339 consolidation, but also its mechanistic role in regulation of mood and affect. It will also have
340 specific implications for treating disorders where fear is dysregulated or misattributed, including
341 anxiety and panic disorders, acute stress disorder, and PTSD.

342

343 **Materials and Methods**

344

345 **Animal handling and husbandry**

346 All animal procedures were approved by the University of Michigan Institutional Animal
347 Care and Use Committee. With the exception of constant dark following tamoxifen
348 administration, mice were kept on a 12 h:12 h light:dark (LD) cycle, and were given food and
349 water *ad lib* throughout the entirety of the study. Following surgical procedures, and during
350 habituation prior to cued conditioning, mice were individually housed in standard caging with
351 beneficial environmental enrichment (nesting material, manipulanda, and/or novel foods).

352

353 **Visually-cued fear conditioning**

354 For 3 days prior to conditioning, mice were habituated to 5 min/day of gentle handling.
355 Following the habituation period, at ZT0, mice underwent visually-cued fear conditioning in a
356 novel arena (context A). They were allowed 2 minutes to acclimate to the arena. They then
357 experienced 3 pairings of a 30-s visual stimulus (presented simultaneously on 4 LED monitors
358 surrounding the arena) co-terminating with a 2-s 0.75 mA foot shock. These pairings were
359 divided with a 60-s intertrial interval. Each visual stimulus consisted of a 1 Hz phase-reversing
360 oriented grating (X°) with a spatial frequency of 0.05 cycles/degree and contrast of 100%.

361 Following conditioning, C57BL/6J mice (Jackson) used for experiments outlined in
362 **Figure 1** were returned to their home cage and were either allowed 12 h *ad lib* sleep, or were
363 sleep deprived (SD) using gentle handling (i.e., cage tapping, nest disturbance, and light touch
364 with a cotton-tipped applicator to cause arousal from sleep) for 6 h, after which they were
365 allowed 6 h *ad lib* sleep. All transgenic mice (see below) with data shown in **Figures 2, 3, and 7**
366 were allowed *ad lib* sleep in their home cage following conditioning.

367 At ZT12 (i.e., 12 h following conditioning) mice were placed in a dissimilar novel context
368 B for cued fear memory testing. Context B differed from context A (used during conditioning),
369 with the two arenas having a unique odor, shape, size, floor texture, and lighting condition.
370 During testing, mice were exposed to two distinct oriented grating stimuli (X° and Y°) to assess
371 cue discrimination. At the start of each test, mice were allowed 3 min to acclimate to the arena,
372 after which an oriented grating either the same as the shock cue (X°) or distinct (Y°) was
373 presented for 3 min followed by 1 min of post stimulus arena exploration. A minimum of thirty
374 minutes were left between the presentations of the tests.

375 Freezing responses were quantified for each grating stimulus using previously-
376 established criteria⁴⁴. For each test, two scorers blinded to behavioral condition quantified
377 periods of immobility during presentation of grating stimuli that included fear features such as
378 hyperventilation and rigid posture. Freezing during presentation of the two gratings was
379 compared to calculate a discrimination index: (percent freezing during shock [X°]
380 stimulus)/(percent freezing during shock [X°] stimulus + percent freezing during neutral [Y°]
381 stimulus).

382 To test for time-of-day effects on visually-cued fear memory recall (**Supplemental**
383 **Figure 2**), additional cohorts of mice were trained at ZT0 as described above, and tested at 12,
384 24, or 36 h later.

385

386 **Genetic tagging of orientation-selective V1 neurons**

387 Prior to all procedures for targeted recombination in visual engram neurons, mice were
388 habituated for 3 days to gentle handling procedures. After habituation, at ZT0, the mice were
389 placed in this square arena surrounded by 4 LED monitors. Each monitor presented a single-
390 orientation (X°) phase-reversing grating stimulus (1 Hz, 0.05 cycles/degree, 100% contrast) for
391 30 min (or, for negative controls shown in **Figure 2**, a dark screen). Immediately after stimulus
392 or dark screen presentation, mice received an i.p. injection of tamoxifen (100mg/kg in 95% corn
393 oil/ 5% ethanol), and were placed in complete darkness for the next 3 d to prevent further
394 visually-driven recombination in V1. Following 3 d of constant dark housing, mice were returned
395 to a normal 12 h:12 h LD cycle for 7 d prior to further experiments. cfos-CRE^{ER} mice (Guenther
396 et al 2013; B6.129(Cg)-Fos^{tm1.1(cre/ERT2)Luo/J}; Jackson) crossed to either B6.Cg-
397 Gt(ROSA)26Sor^{tm9(CAG-tdTomato)Hze/J}, B6.Cg-Gt(ROSA)26Sor^{tm32(CAG-COP4*H134R/EYFP)Hze/J}, or B6.Cg-
398 Gt(ROSA)26Sor^{tm40.1(CAG-aop3/EGFP)Hze/J} (Jackson) mice to induce CRE recombinase-mediated
399 expression of tdTomato, ChR2, or ArchT.

400

401 **Histology and immunohistochemistry**

402 At the conclusion of each experiment, mice were deeply anesthetized with pentobarbital,
403 and transcardially perfused with saline and 4% paraformaldehyde. Brains were dissected, post-
404 fixed, cryoprotected in 30% sucrose, and cryosectioned at 50 μ m. Transgene expression in V1
405 was verified for all experiments using CRE-dependent transgenic lines prior to subsequent data
406 analysis. For electrophysiological recordings in V1, electrode placement was verified prior to
407 data analysis. Immunohistochemistry for cFos was carried out using rabbit-anti-cfos 1:1000
408 (Abcam; ab190289) and secondary donkey-anti-rabbit conjugated to Alexa Fluor 405 (1:200;
409 Abcam; ab175651); coronal sections containing V1 were mounted using Fluoromount-G
410 (Southern Biotech). Co-labeling of tdTomato and anti-cFos was quantified using Image J
411 software in 6 sections containing V1 from each mouse by a scorer blinded to animal condition.
412 Average co-labeling values for each mouse are reported in **Figures 2** and **4**.

413

414 **V1 visual response recordings, optogenetic manipulations, and data analysis**

415 For anesthetized recordings of V1 neurons' visual responses and firing, mice were
416 anesthetized using a combination of isoflurane (0.5-0.8%) and 1 mg/kg chlorprothixene (Sigma).
417 Data was acquired using a 32-channel Plexon Omniplex recording system, using previously-
418 described methods^{20,22}. A 2-shank, linear silicon probe (250 μ m spacing between shanks) with
419 25 μ m inter-electrode spacing (16 electrodes/shank; Cambridge Neurotech) was slowly
420 advanced into V1 until stable recordings (with consistent spike waveforms continuously present
421 for at least 30 min prior to baseline recording) were obtained. Orientation tuning curves for
422 recorded neurons were generated by presenting a series of 8 full-field phase-reversing oriented
423 gratings (0, 22.5, 45, 67.5, 90, 112.5, 135, or 157.5 degrees from horizontal, 1 Hz, 0.05
424 cycles/degree, 100% contrast, 10 s duration) and a blank screen (to evaluate spontaneous
425 activity) presented repeatedly (4-8 times each) in an interleaved manner.

426 For recordings during rhythmic optogenetic activation of X° -activated V1 neurons in
427 ChR2-expressing mice (**Figure 5**) tuning curves were generated: 1) at baseline, 2) after a 20-30
428 min period without optogenetic manipulation, and 3) after a 20-30 min period of 1 Hz
429 optogenetic stimulation. Optogenetic stimulation consisted of blue light pulses (10 ms, 473 nm,

430 10 mW power) delivered at 1 Hz. Only neurons stably recorded throughout all phases of the
431 experiment (shown in **Figure 5A**) were included in firing and visual response analysis.

432 To assess effects of optogenetic inhibition of X°-activated V1 neurons in ArchT-
433 expressing mice (**Figure 6**) recordings consisted of a 30-min spontaneous activity recording
434 with no manipulation, a 30-min recording with periodic inhibition (532 nm green light, 15 mW,
435 delivered in cycles of 5 s on, followed by a 500 ms offramp and a 1-s off period). Following
436 these recordings, two orientation tuning curves were generated for all recorded neurons: 1) a
437 baseline without inhibition, and 2) with inhibition of X°-activated V1 neurons occurring during 10-
438 s presentations of oriented grating stimuli. Only neurons stably recorded throughout all phases
439 of the experiment (shown in **Figure 6A**) were included in firing and visual response analysis.

440 For all recordings, stable single units were isolated using PCA-based analysis and
441 MANOVA-based cluster separation, implemented using Offline Sorter software (Plexon) and
442 previously-described methods^{20,22}. Units that could not be reliably discriminated, or had
443 refractory period violations in their spiking patterns, were eliminated from subsequent analyses.
444 Changes in orientation tuning were assessed relative to the orientation of the TRAPed
445 ensemble (X°), based on neurons mean firing rate responses to gratings of different
446 orientations. For each tuning curve, an orientation preference index (OPI) was calculated for X°
447 and the orthogonal stimulus orientation (X°/X+90°), as described previously^{20,27,28}. % changes in
448 OPI (across optogenetic stimulation or control conditions) were calculated as $[(OPI^{pre}-$
449 $OPI^{post})/OPI^{pre}] * 100$. Firing responses of neurons during rhythmic optogenetic stimulation in
450 ChR2-expressing mice was assessed from Z-scored perievent rasters centered on blue light
451 onset; significance of time-locked excitation or inhibition was calculated based on positive or
452 negative Z-score deviations beyond the 99% confidence interval (Neuralynx; Plexon). Changes
453 in firing during optogenetic inhibition in ArchT-expressing mice were calculated for each neuron
454 within the inhibition recording period, by comparing mean firing rate during the last 1.5 s of each
455 green light delivery period with mean firing rate during the subsequent 500 ms offramps and 1-s
456 off period.

457 Power spectral density for local field potentials was detrended using NeuroExplorer
458 software (Plexon) with a single taper Hann Windowing Function with 50% window overlap.
459 These were averaged across all active electrodes on each silicon probe shank. Distributions of
460 power (between 0 and 20 Hz) were compared statistically using KS tests.

461

462 **Surgical procedures**

463 For V1 optical fiber implantation, mice were anesthetized using 1-2% isoflurane. Optical
464 fibers (0.5 NA, 300 um core, ThorLabs) were positioned bilaterally at the surface of V1 at a 80
465 degree angle relative to the cortical surface (2.9 mm posterior, 2.7 mm lateral). Implants were
466 secured to the skull with an anchor screw positioned anterior to bregma, using Loctite adhesive.
467 For EEG/EMG recordings to differentiate sleep states, in addition to bilateral V1 optical fibers,
468 mice received an EEG screw over V1 (2.9 mm posterior, 2.3 mm lateral), a reference screw
469 over the cerebellum, and an additional EMG electrode in nuchal muscle. Mice were allowed 10
470 days of postoperative recovery before procedures to induce transgene expression in V1.

471

472 **Optogenetic manipulations in behaving animals**

473 Two cohorts of implanted mice, expressing ChR2 in the TRAPed ensemble, were used
474 to test perception of optogenetic activation of this cell population. Prior to behavioral training and
475 testing, these mice were habituated to handling and tethering (for light delivery to V1)
476 procedures for 3 days. The first cohort underwent cued fear conditioning as described above in
477 context A at ZT0, with 30-s blocks of rhythmic light delivery to V1 (1 Hz, 10 mW, 10 ms pulses)
478 serving as a proxy shock cue (i.e., substituting for visual oriented grating presentation).
479 Following 3 optogenetic stimulation-shock pairings, these mice were returned to their home
480 cages and allowed *ad lib* sleep until ZT12. At ZT 12, they were placed in context B and freezing
481 responses were assessed for visual presentation of both the same orientation as the TRAPed
482 ensemble (X°) and an alternate orientation (Y°), as described above. A second cohort of mice
483 underwent visually-cued fear conditioning to the same angle as the TRAPed ensemble (X°) in
484 context A at ZT0. After conditioning, they were returned to their home cage for *ad lib* sleep. At
485 ZT12, they were tested in context B, where freezing behavior was assessed before, during, and
486 after a period of 1 Hz light delivery to V1 (3 min before, 3 min during, and 1 min after).

487 To assess effects of sleep-targeted inhibition of visual engram neurons, 10 days after
488 EEG/EMG and optical fiber implantation, mice underwent procedures to induce expression of
489 ArchT in the TRAPed orientation-specific ensemble. Following 3 days of habituation to handling
490 and tethering (for light delivery to V1 and EEG/EMG recording), these mice underwent 12 h
491 sleep/wake baseline recordings, starting at ZT0. The next day, mice underwent visually-cued
492 fear conditioning at ZT0, using either the same orientation as the TRAPed ensemble (X°) or an
493 alternate orientation (Y°) as a cue for foot shock. They were then returned to their home cage
494 for *ad lib* sleep. For the first 6 h post-conditioning, a subset of mice expressing ArchT underwent
495 periodic optogenetic inhibition targeted to both NREM and REM sleep. The state targeting was
496 based on EEG signals, EMG signals, and the animal's behavior. A control group of mice which
497 were not expressing ArchT underwent the same light delivery and recording procedures. At
498 ZT12, all mice were placed in context B to assess freezing responses to both X° and Y° oriented
499 gratings, as described above.

500 EEG and EMG signals were used offline to classify each 10-s interval of baseline and
501 post-conditioning recording periods as either wake, NREM, or REM sleep, using custom
502 MATLAB software^{20,22}. Additionally microarousals (periods of non-oscillatory activity between
503 periods of NREM) as small as 5 s were identified as wake. Mean power spectral density was
504 calculated separately within REM, NREM, and wake for each phase of recording, and within and
505 outside of periods of light delivery to V1, as described previously²⁰. The power spectra were
506 calculated as percent of the total spectral power.

507

508 **Statistical methods**

509 All statistical analyses were done using GraphPad Prism. Prior to making comparisons
510 across values, the normality of distributions was tested using the D'Agostino-Pearson omnibus
511 k_2 test. Nonparametric tests were used when data distributions were non-normal or when n
512 values were too low to test normality. If the data involved multiple data measurements from one
513 animal (e.g. multiple images taken from the same animal for immunohistochemistry), nested
514 statistics were used. All statistical tests were two-tailed. For each specific data set the statistical

515 tests used are listed in the **Results** section. p -values are represented as * $p < 0.05$, ** $p < 0.01$,
516 *** $p < 0.001$, **** $p < 0.0001$

517

518 **Data availability**

519 All relevant data and analysis tools are available upon reasonable request from the
520 authors.

521

522 **Code availability**

523 Any MATLAB codes used in analysis are available from the authors upon reasonable
524 request.

525

526

527

528 **Figure Legends:**

529

530 **Figure 1. Consolidation of visually-cued fear memory is enhanced by post-conditioning**
531 **sleep. (a)** At ZT0, mice underwent three stimulus-shock pairings in context A. After either 12 h
532 of *ad lib* sleep or 6 h sleep deprivation (SD) followed by 6 h *ad lib* sleep, mice were exposed to
533 the shock cue (X° grating) and a neutral cue (Y° grating) in context B. **(b)** Freezing behavior of
534 the mice during the ZT12 test (Sleep: $n = 15$ - sleep, SD: $n = 14$; males - solid symbols, females
535 - open symbols). Mice allowed to sleep froze significantly more to the shock cue than mice who
536 were sleep deprived (** indicates $p = 0.002$, Holm-Sidak *post hoc* test). Both freely-sleeping and
537 SD mice showed higher freezing in response to the shock cue (**** indicates $p < 0.0001$, *
538 indicates $p = 0.03$, Holm-Sidak *post hoc* test; two-way RM ANOVA: main effect of sleep
539 condition, $F = 6.9$, $p = 0.014$, main effect of orientation, $F = 28.5$, $p < 0.001$, sleep x orientation
540 interaction, $F = 4.4$, $p = 0.047$). **(c)** Freezing behavior quantified a discrimination index
541 [$X^\circ/(X^\circ+Y^\circ)$] for each mouse and compared to chance performance (* indicates $p = 0.049$, **
542 indicates $p = 0.0003$, Wilcoxon signed rank test vs. chance).

543

544 **Figure 2. TRAP labels orientation-selective V1 ensembles. (a)** *cfos::tdTom* mice were
545 presented with either a dark screen or an oriented grating (X°) and were then injected with
546 tamoxifen prior to 3 d of housing in complete darkness. **(b-c)** Representative V1 tdTomato
547 labelling quantified 11 d after tamoxifen administration. **** indicates $p = 0.0001$ ($t = 7.07$, $DF =$
548 8) for dark screen vs. X° , nested t-test ($n = 5$ mice/condition) **(d)** Prior to tissue harvest, mice
549 were either re-exposed to gratings of the same orientation (X°) or an alternate orientation (Y°).
550 **(e-f)** Representative images showing overlap of tdTomato (red) and cFos protein (cyan). An
551 example of colocalization within a neuron (quantified in **f**) is indicated with a white arrow for
552 each image in the inset. ** indicates $p = 0.009$ ($t = 3.22$, $DF = 10$), nested t-test ($n = 5$ mice for
553 X° , $n = 6$ mice for Y°).

554

555 **Figure 3. Optogenetic stimulation of TRAPed V1 neurons mimics visual experience. (a)**
556 *cfos::Chr2* mice with bilateral V1 fiber optics had recombination induced to a specific angle
557 (X°). 11 days later, visual behavior was run. **(b-c)** At ZT 0, the mice received bilateral V1
558 optogenetic stimulation paired with foot shocks in lieu of the oriented grating visual stimuli used
559 for cued conditioning in **Figure 1**. At ZT 12, the mice were presented with the same oriented
560 grating used for TRAP (X°) and an alternate orientation (Y°). Optogenetically-cued conditioning
561 resulted in higher subsequent cued freezing responses to X° relative to Y° ($n = 10$ mice; $p =$
562 0.008 [$t = 3.38$, $DF = 9$], ratio paired t-test). **(d-e)** At ZT0, a second cohort of mice underwent
563 visually-cued fear conditioning to the same orientation as the TRAPed ensemble. At ZT12, the
564 mice received optogenetic stimulation in place of a visual test. Freezing behavior was higher
565 during optogenetic stimulation than before or after stimulation ($n = 5$ mice; pre vs. stim - $p =$
566 0.003 [$t = 7.30$, $DF = 4$, stim vs. post - $p = 0.003$ [$t = 7.85$, $DF = 4$], Holm-Sidak *post hoc* test,
567 one-way RM ANOVA).

568

569 **Figure 4. TRAPed V1 neurons selective for the conditioned stimulus are reactivated in**
570 **post-conditioning sleep. (a)** *cfos::tdTom* mice had recombination induced to a specific angle
571 (X°). 11 days later, they were cue conditioned to either the same angle as induction (X° ; $n = 7$

572 mice) or an alternate angle (Y° ; $n = 4$ mice). All mice were allowed 4.5 h of post-conditioning *ad*
573 *lib* sleep prior to tissue harvest. **(b-c)** Representative images showing overlap of cFos
574 expression (cyan) with tdTomato (red). The boxed region is magnified as an inset with an arrow
575 indicating an overlapping neuron. Expression of cFos in tdTomato-labelled cells was greater for
576 mice conditioned to the same orientation used for TRAP labelling (* indicates $p = 0.025$ [$t =$
577 2.69 , $DF = 9$], nested t-test).

578

579 **Figure 5. Offline reactivation of orientation-selective TRAPed V1 neurons alters**
580 **orientation representations in V1. (a)** *cfos::ChR2* mice were presented with an oriented
581 grating (X°) for TRAP. 11 days later, orientation tuning was measured repeatedly for V1 neurons
582 recorded from anesthetized mice: at baseline, after a 20-30 min period without optogenetic
583 stimulation, and after a 20-30 min period with 1 Hz light delivery. **(b)** Representative rasters and
584 perievent histograms for 4 simultaneously-recorded neurons, showing diverse firing responses
585 during optogenetic stimulation. **(c)** The majority of stably-recorded V1 neurons were reliably
586 activated following light pulses, with variable lag times. A small proportion were inhibited by light
587 delivery, and the remaining neurons were not affected ($n = 62$ neurons from 5 mice, total). **(d)**
588 Power spectra for V1 LFPs showed no significant effect on ongoing rhythmic activity (*N.S.*, K-S
589 test, $n = 5$ mice) **(e-f)** After optogenetic stimulation, neurons that were not activated following
590 light pulses showed no change in orientation preference (*N.S.*, nested t-test, $n = 32$ neurons
591 from 5 mice). In contrast, activated neurons showed increased firing rate responses for gratings
592 of the same orientation (X°) used for TRAP. (** indicates $p = 0.002$ [$t = 3.27$, $DF = 62$], nested t-
593 test, $n = 30$ neurons from 5 mice).

594

595 **Figure 6. Optogenetic inhibition of orientation-selective TRAPed V1 ensembles alters**
596 **orientation preference in surrounding V1 neurons. (a)** *cfos::ArchT* mice were presented with
597 an oriented grating (X°) for TRAP. 11 days later, V1 neurons were recorded from anesthetized
598 mice across 30 minutes of optogenetic inhibition, and 30 minutes without inhibition. Afterward,
599 orientation preference was assessed without optogenetic inhibition (no laser) and with inhibition.
600 **(b)** Representative rasters and perievent histograms for 4 simultaneously-recorded neurons,
601 showing diverse firing responses during optogenetic inhibition. **(c)** Distributions of stably-
602 recorded V1 neurons which were significantly inhibited, activated following light pulses, or
603 unaffected by light delivery ($n = 58$ neurons from 5 mice). **(d)** Power spectra for V1 LFPs
604 showed no significant change in rhythmic activity during periods of inhibition (*N.S.*, K-S test, $n =$
605 5 mice). **(e-f)** During optogenetic inhibition, neurons that showed no decrease in firing rate
606 showed no change in orientation preference (*N.S.*, nested t-test, $n = 32$ neurons from 5 mice).
607 In contrast, neurons that were inhibited showed a reduced preference for gratings of the same
608 orientation (X°) used for TRAP (** indicates $p = 0.007$ [$t = 3.65$, $DF = 8$, nested t-test, $n = 26$
609 neurons from 5 mice).

610

611 **Figure 7. Sleep-specific inhibition of a V1 engram disrupts visually-cued fear memory**
612 **consolidation. (a)** *cfos::ArchT* mice implanted with bilateral V1 optical fibers and EEG/EMG
613 electrodes were presented with X° for TRAP. 11 days later, mice were conditioned using either
614 the same orientation (X°) or an alternate orientation (Y°) as the shock cue. Post-conditioning,
615 the mice slept, with sleep-specific inhibition during the first 6h. **(b)** No-inhibition (non-opsin-

616 expressing) controls and mice cued to Y° with subsequent optogenetic inhibition showed higher
617 freezing responses to the shock cue vs. the neutral cue (two-way RM ANOVA: main effect of
618 optogenetic manipulation condition, $F = 9.9$, $p < 0.001$, main effect of orientation, $F = 9.0$, $p =$
619 0.007 , optogenetic condition x orientation interaction, $F = 7.9$, $p = 0.003$, no-inhibition control - p
620 $= 0.02$, Y°-cued inhibition - $p < 0.001$, Holm-Sidak *post hoc* test). In contrast, mice cued to X°
621 with subsequent optogenetic inhibition did not differ in freezing responses to the shock cue vs.
622 the neutral cue (*N.S.*, Holm-Sidak *post hoc* test). Mice cued to either X° or Y° with subsequent
623 inhibition showed higher freezing responses to both cues relative to no-inhibition controls,
624 indicative of generalization. **(c)** Controls and mice cued to Y° show significant discrimination,
625 while mice cued to X° did not (* indicates $p = 0.016$ for both no-inhibition control and Y°-cued
626 with inhibition; Wilcoxon signed rank test).
627

628 **Extended Data Figure Legends:**

629

630 **Figure S1. Both female and male mice show deficits in visually-cued fear memory**
631 **following post-conditioning sleep deprivation. (a)** Male mice allowed *ad lib* sleep following
632 conditioning froze significantly more to the shock cue (X°) than mice who were sleep deprived (*
633 indicates $p = 0.01$, Holm-Sidak *post hoc* test). Freely sleeping male mice froze significantly
634 more in response the shock cue than a neutral cue (***) indicates $p = 0.001$, Holm-Sidak *post*
635 *hoc* test). **(b)** Sleeping, but not sleep deprived, male mice showed discrimination for shock vs.
636 neutral cues above chance (* indicates $p = 0.02$, Wilcoxon signed rank test). **(c)** Female mice
637 who were allowed *ad lib* sleep also showed higher freezing responses to the shock cue than the
638 neutral cue (** indicates $p = 0.007$, Holm-Sidak *post hoc* test). **(d)** Female mice allowed *ad lib*
639 sleep showed discrimination in their responses to shock vs. neutral cues, while sleep deprived
640 female mice did not (* indicates $p = 0.02$, Wilcoxon signed rank test vs chance).

641

642 **Figure S2. Discrimination of fear cues at testing follows a diurnal pattern. (a)** ZT12 cued
643 fear test performance, carried out on the day of conditioning. Sleeping mice showed higher
644 freezing in response to the shock cue than SD mice (* indicates $p = 0.01$, Holm-Sidak *post hoc*
645 test). Sleeping mice froze more in response to presentation of the shock cue than the neutral
646 cue (***) indicates $p = 0.001$, Holm-Sidak *post hoc* test). **(b)** Sleeping mice, but not SD mice,
647 showed freezing response discrimination between shock and neutral cues (* indicates $p = 0.02$,
648 Wilcoxon signed rank test vs chance) **(c)** ZT0 cued fear test performance, carried out 24 h
649 following conditioning. There were no differences within groups or across groups (*N.S.*, Holm-
650 Sidak *post hoc* test). **(d)** Neither group discriminated between shock and neutral cues beyond
651 chance (*N.S.*, Wilcoxon signed rank test vs chance). **(e)** ZT12 cued fear test performance,
652 carried out on the day following conditioning. Freely sleeping mice showed greater freezing in
653 response to the shock cue than SD mice (* indicates $p = 0.01$, Holm-Sidak *post hoc* test).
654 Sleeping mice froze more in response to presentation of the shock cue vs. the neutral cue (***)
655 indicates $p < 0.001$, Holm-Sidak *post hoc* test). **(f)** Mice allowed *ad lib* sleep (but not SD mice)
656 showed discrimination of freezing responses to shock vs. neutral cues above chance (*
657 indicates $p = 0.03$, Wilcoxon signed rank test vs. chance).

658

659 **Figure S3. State-specific targeting of optogenetic inhibition.** There were no significant
660 differences in state coverage between different experimental groups (*N.S.*, two-way RM ANOVA
661 for $n = 8$ no-opsin [no-inhibition] control mice, $n = 8$ mice cued to X° with subsequent inhibition,
662 $n = 7$ mice cued to Y° with subsequent inhibition). In each group, light was delivered to V1
663 throughout most of REM sleep ($93 \pm 3\%$, $96 \pm 1\%$, and $96 \pm 3\%$ of total REM, respectively) and
664 NREM sleep ($69 \pm 3\%$, $75 \pm 4\%$, and $79 \pm 3\%$ of total NREM, respectively) were covered. In
665 each group there was a small amount of light delivery during wake, primarily during
666 microarousals ($19 \pm 2\%$, $15 \pm 2\%$, and $22 \pm 3\%$ of total wake, respectively).

667

668 **Figure S4. Sleep architecture and power during baseline and optogenetic inhibition. (a)**
669 Representative traces of EEG classified as NREM sleep, REM sleep, and wake. **(b-d)** Percent
670 of recording time spent in each state across recording periods and experimental groups. There
671 were no significant differences in sleep time between groups (*N.S.*, two-way RM ANOVA). **(e-g)**

672 Average bout length for each state across recording times and across experimental groups.
673 There were no significant differences between groups (*N.S.*, two-way RM ANOVA). **(h-j)**
674 Average power within NREM delta (0.5-4 Hz), NREM spindle (12-15 Hz), and REM theta (4-12
675 Hz) frequency bands across recording periods and experimental groups. There were no
676 significant differences between groups (*N.S.*, two-way RM ANOVA).
677
678
679
680
681
682

683

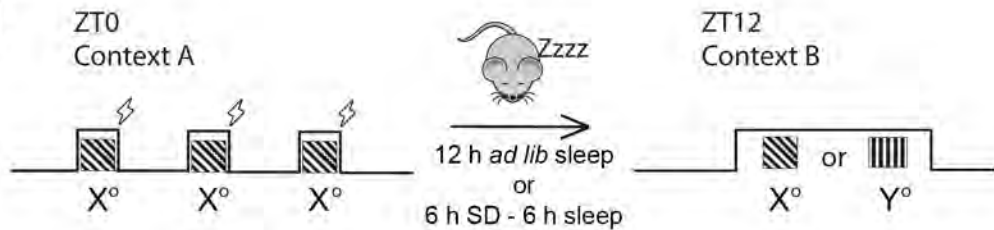
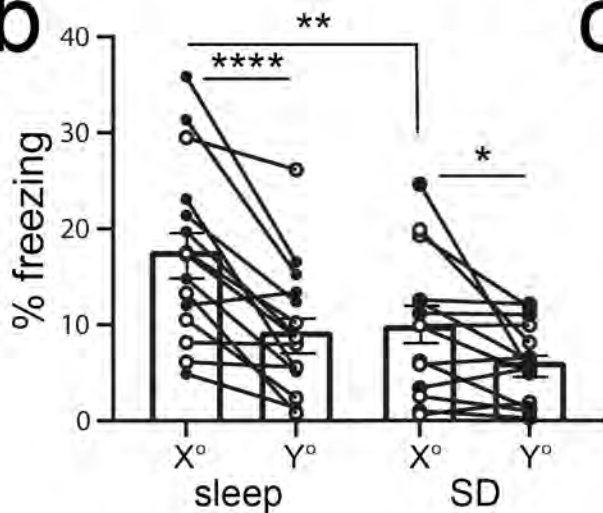
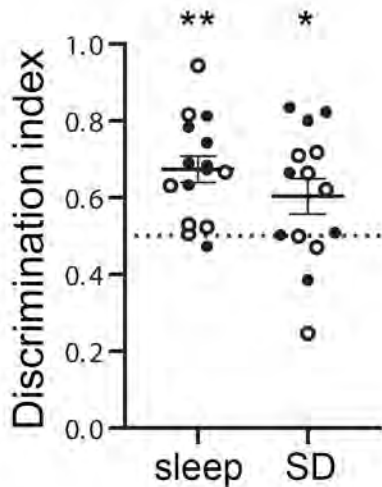
684 **References Cited:**

685

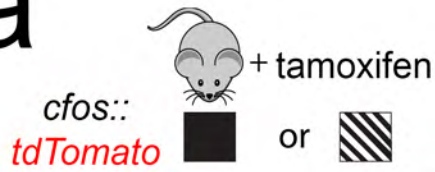
- 686 1 Pavlides, C. & Winson, J. Influences of hippocampal place cell firing in the awake state
687 on the activity of these cells during subsequent sleep. *Journal of Neuroscience* **9**, 2907-
688 2918 (1989).
- 689 2 Wilson, M. A. & McNaughton, B. L. Reactivation of hippocampal ensemble memories
690 during sleep. *Science* **265**, 676-682 (1994).
- 691 3 Kudrimoti, H. S., Barnes, C. A. & McNaughton, B. L. Reactivation of hippocampal cell
692 assemblies: Effects of behavioral state, experience and EEG dynamics. *Journal of*
693 *Neuroscience* **19**, 4090-4101 (1999).
- 694 4 Skaggs, W. E. & McNaughton, B. L. Replay of neuronal firing sequences in rat
695 hippocampus during sleep following spatial experience. *Science* **271**, 1870-1873 (1996).
- 696 5 Lee, A. K. & Wilson, M. A. Memory of sequential experience in the hippocampus during
697 slow wave sleep. *Neuron* **36**, 1183-1194 (2002).
- 698 6 Louie, K. & Wilson, M. A. Temporally structured replay of awake hippocampal ensemble
699 activity during rapid eye movement sleep. *Neuron* **29**, 145-156 (2001).
- 700 7 Ji, D. & Wilson, M. A. Coordinated memory replay in the visual cortex and hippocampus
701 during sleep. *Nat Neurosci* **10**, 100-107 (2007).
- 702 8 Euston, D. R., Tatsuno, M. & McNaughton, B. L. Fast-forward playback of recent
703 memory sequences in prefrontal cortex during sleep. *Science* **318**, 1147-1150 (2007).
- 704 9 Peyrache, A., Khamassi, M., Benchenane, K., Wiener, S. I. & Battaglia, F. Replay of
705 rule-learning related neural patterns in the prefrontal cortex during sleep. *Nat Neurosci*
706 **12**, 919-926 (2009).
- 707 10 Hoffman, K. L. & McNaughton, B. L. Coordinated reactivation of distributed memory
708 traces in primate cortex. *Science* **297**, 2070-2073 (2002).
- 709 11 Dave, A. S. & D., M. Song replay during sleep and computational rules of sensorimotor
710 vocal learning. *Science* **290**, 812-816 (2000).
- 711 12 Pennartz, C. M. A. *et al.* The Ventral Striatum in Off-Line Processing: Ensemble
712 Reactivation during Sleep and Modulation by Hippocampal Ripples. *J.Neurosci.* **24**,
713 6446-6456 (2004).
- 714 13 Rothschild, G., Eban, E. & Frank, L. M. A cortical–hippocampal–cortical loop of
715 information processing during memory consolidation. *Nat Neurosci* **20**, 251-259 (2017).
- 716 14 Puentes-Mestri, C., Roach, J., Niethard, N., Zochowski, M. & Aton, S. J. How rhythms of
717 the sleeping brain tune memory and synaptic plasticity. *Sleep* **42**, pii: zsz095,
718 doi:10.1093/sleep/zsz095 (2019).
- 719 15 Puentes-Mestri, C. & Aton, S. J. Linking network activity to synaptic plasticity during
720 sleep: hypotheses and recent data. *Frontiers in Neural Circuits* **11**, doi:
721 10.3389/fncir.2017.00061 (2017).
- 722 16 Girardeau, G., Benchenane, K., Wiener, S. I., Buzsaki, G. & Zugaro, M. B. Selective
723 suppression of hippocampal ripples impairs spatial memory. *Nat Neurosci* **12**, 1222-
724 1223 (2009).
- 725 17 Ego-Stengel, V. & Wilson, M. A. Disruption of ripple-associated hippocampal activity
726 during rest impairs spatial learning in the rat. *Neurosci Res* **20**, 1-10 (2011).
- 727 18 Gridchyn, I., Schoenenberger, P., O'Neill, J. & Csicsvari, J. Assembly-Specific
728 Disruption of Hippocampal Replay Leads to Selective Memory Deficit. *Neuron* pii:
729 **S0896-6273(20)30047-7**, doi:10.1016/j.neuron.2020.01.021. (2020).
- 730 19 van de Ven, G., Trouche, S., McNamara, C., Allen, K. & Dupret, D. Hippocampal Offline
731 Reactivation Consolidates Recently Formed Cell Assembly Patterns during Sharp Wave-
732 Ripples. *Neuron* **92**, 968-974 (2016).

- 733 20 Durkin, J. *et al.* Cortically coordinated NREM thalamocortical oscillations play an
734 essential, instructive role in visual system plasticity. *Proceedings National Academy of*
735 *Sciences* **114**, 10485-10490 (2017).
- 736 21 Ognjanovski, N., Broussard, C., Zochowski, M. & Aton, S. J. Hippocampal Network
737 Oscillations Rescue Memory Consolidation Deficits Caused by Sleep Loss. *Cereb.*
738 *Cortex* **28**, 3711-3723, doi:10.1093/cercor/bhy174 (2018).
- 739 22 Ognjanovski, N. *et al.* Parvalbumin-expressing interneurons coordinate hippocampal
740 network dynamics required for memory consolidation. *Nature Communications* **8**, 15039
741 (2017).
- 742 23 Xia, F. *et al.* Parvalbumin-positive interneurons mediate neocortical-hippocampal
743 interactions that are necessary for memory consolidation. *eLife* **6**, e27868 (2017).
- 744 24 Liu, X. *et al.* Optogenetic stimulation of a hippocampal engram activates fear memory
745 recall. *Nature* **484**, 381-385 (2012).
- 746 25 Ramirez, S. *et al.* Creating a false memory in the hippocampus. *Science* **341**, 387-391
747 (2013).
- 748 26 Clawson, B. C. *et al.* Sleep Promotes, and Sleep Loss Inhibits, Selective Changes in
749 Firing Rate, Response Properties and Functional Connectivity of Primary Visual Cortex
750 Neurons. *Frontiers in Systems Neuroscience* **12**, 40, doi:doi: 10.3389/fnsys.2018.00040
751 (2018).
- 752 27 Durkin, J. M. & Aton, S. J. Sleep-dependent potentiation in the visual system is at odds
753 with the Synaptic Homeostasis Hypothesis. *Sleep* (2016).
- 754 28 Aton, S. J., Suresh, A., Broussard, C. & Frank, M. G. Sleep promotes cortical response
755 potentiation following visual experience. *Sleep* **37**, 1163-1170 (2014).
- 756 29 Graves, L. A., Heller, E. A., Pack, A. I. & Abel, T. Sleep deprivation selectively impairs
757 memory consolidation for contextual fear conditioning. *Learn. Mem.* **10**, 168-176 (2003).
- 758 30 Kumar, T. & Jha, S. Sleep deprivation impairs consolidation of cued fear memory in rats.
759 *PLoS One* **7** (2012).
- 760 31 Cai, D., Shuman, T., Harrison, E., Sage, J. & SG, A. Sleep deprivation and Pavlovian
761 fear conditioning. *Learn Mem* **16**, 595-599 (2009).
- 762 32 Ruskin, D., Liu, C., Dunn, K., Bazan, N. & LaHoste, G. Sleep deprivation impairs
763 hippocampus-mediated contextual learning but not amygdala-mediated cued learning in
764 rats. *Eur J Neurosci* **19**, 3121-3124 (2004).
- 765 33 Guenther, C., Miyamichi, K., Yang, H. H., Heller, H. C. & Luo, L. Permanent genetic
766 access to transiently active neurons via TRAP: targeted recombination in active
767 populations. *Neuron* **78**, 773-784 (2013).
- 768 34 Marshel, J. *et al.* Cortical layer-specific critical dynamics triggering perception. *Science*
769 **365**, pii: eaaw5202, doi:10.1126/science.aaw5202 (2019).
- 770 35 Cooke, S. F. & Bear, M. F. Visual experience induces long-term potentiation in the
771 primary visual cortex. *J Neurosci* **30**, 16304-16313 (2010).
- 772 36 Frenkel, M. Y. *et al.* Instructive effect of visual experience in mouse visual cortex.
773 *Neuron* **51**, 339-349 (2006).
- 774 37 Jehee, J. F., Brady, D. K. & Tong, F. Attention improves encoding of task-relevant
775 features in the human visual cortex. *J Neurosci* **31**, 8210-8219 (2011).
- 776 38 Jehee, J., Ling, S., Swisher, J., van Bergen, R. & Tong, F. Perceptual learning
777 selectively refines orientation representations in early visual cortex. *J Neurosci* **32**,
778 16747-16753 (2012).
- 779 39 Adab, H., Popovanov, I., Vanduggel, W. & R, V. Perceptual learning of simple stimuli
780 modifies stimulus representations in posterior inferior temporal cortex. *J Cogn Neurosci*
781 **26**, 2187-2200 (2014).
- 782 40 Adab, H. & Vogels, R. Practicing coarse orientation discrimination improves orientation
783 signals in macaque cortical area V4/. *Curr Biol* **21** (2011).

- 784 41 Ryan, T. J., Roy, D. S., Pignatelli, M., Arons, A. L. & Tonegawa, S. Engram cells retain
785 memory under retrograde amnesia. *Science* **348**, 1007-1013 (2015).
- 786 42 Giri, B., Diba, K., Miyawaki, H., Cheng, S. & Mizuseki, K. Hippocampal reactivation
787 extends for several hours following novel experience. *J Neurosci* **39**, 866-875 (2018).
- 788 43 Bridi, M. C. D. *et al.* Rapid eye movement sleep promotes cortical plasticity in the
789 developing brain. *Science Advances* **1**, 1-8 (2015).
- 790 44 Curzon, P., Rustay, N. & Browman, K. in *Methods of Behavior Analysis in Neuroscience*.
791 (ed J Buccafusco) 19-37 (CRC Press, 2009).
792

a**b****c**

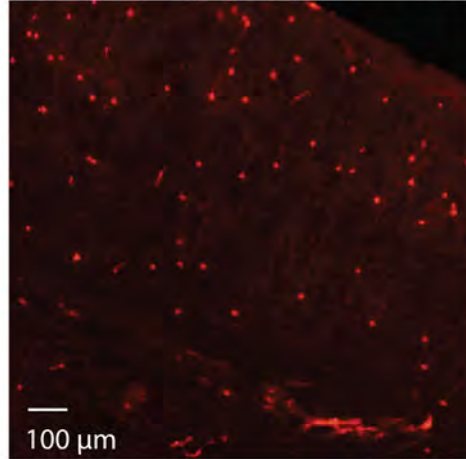
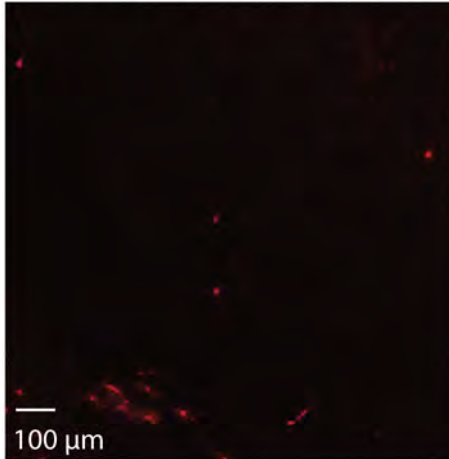
a



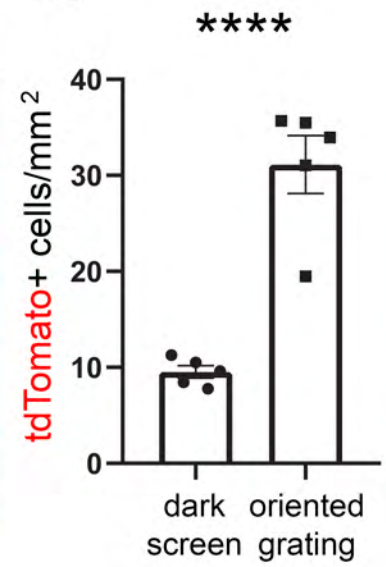
b

■ dark screen

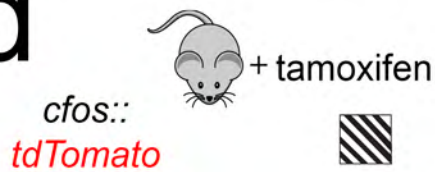
▨ oriented grating



c



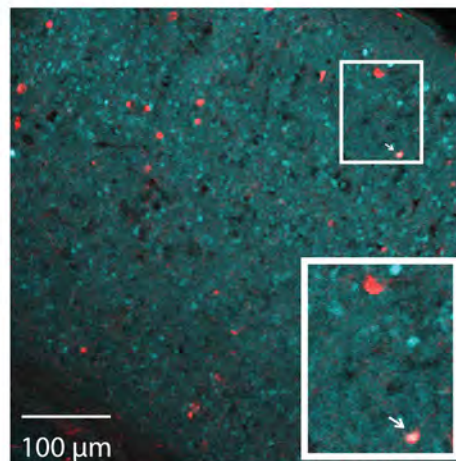
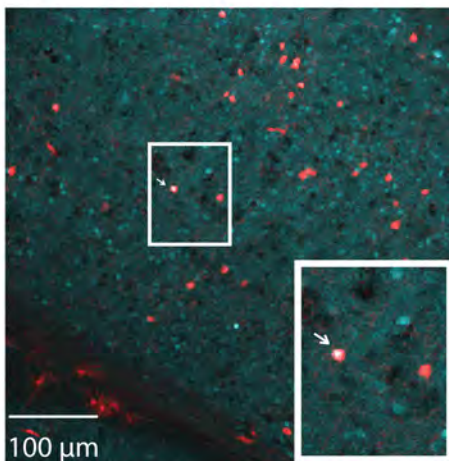
d



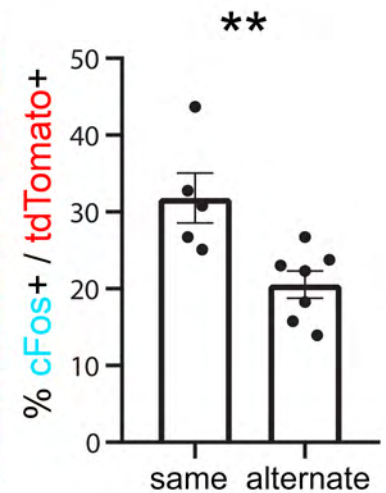
e

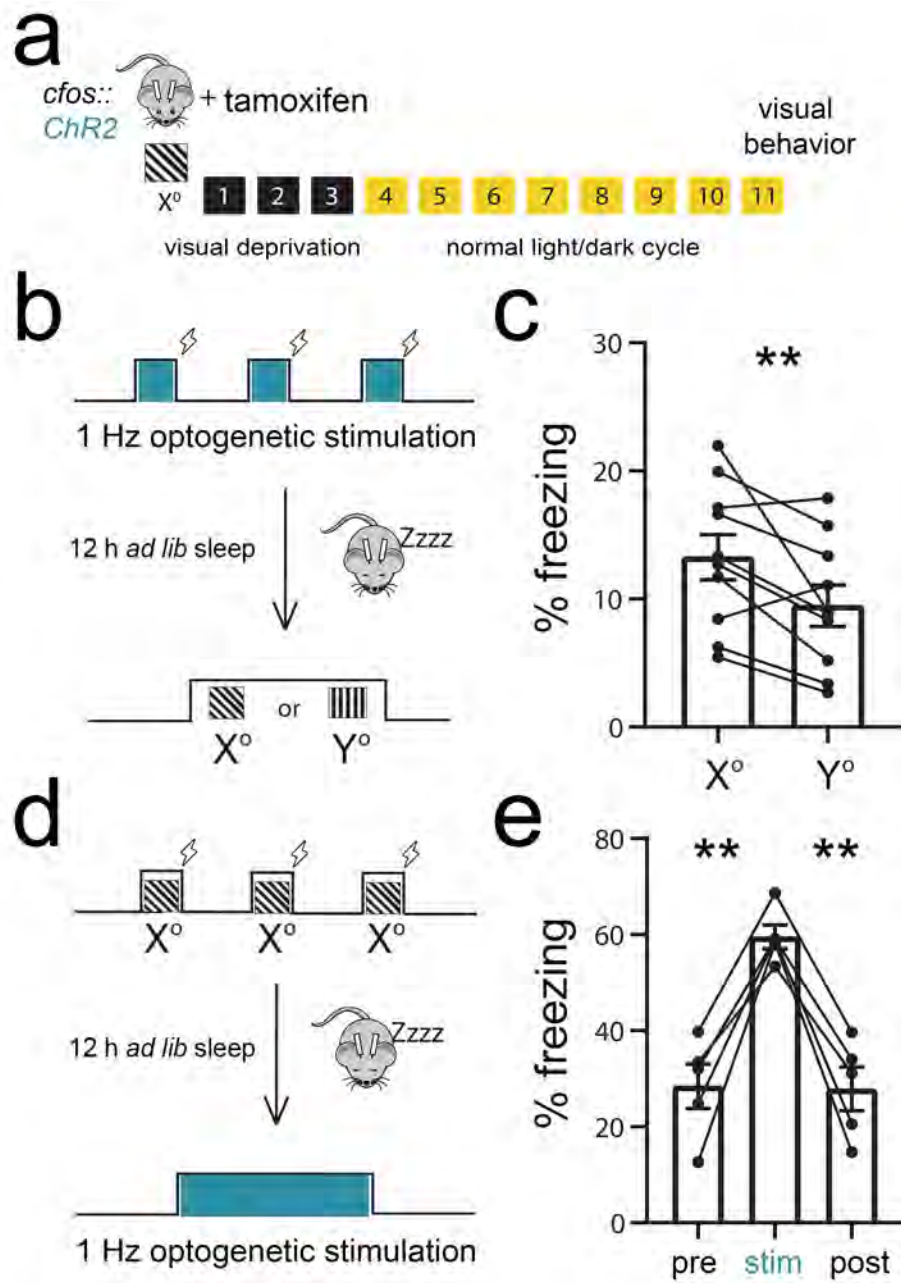
▨ same orientation

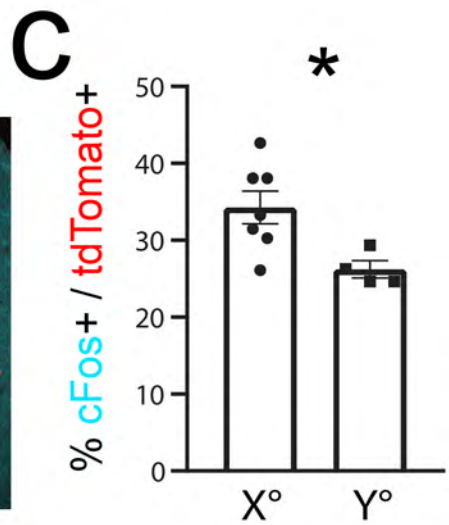
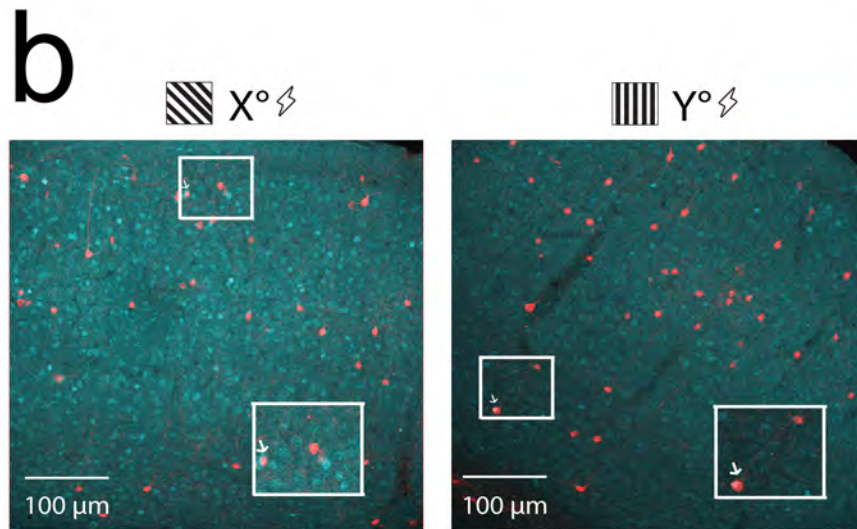
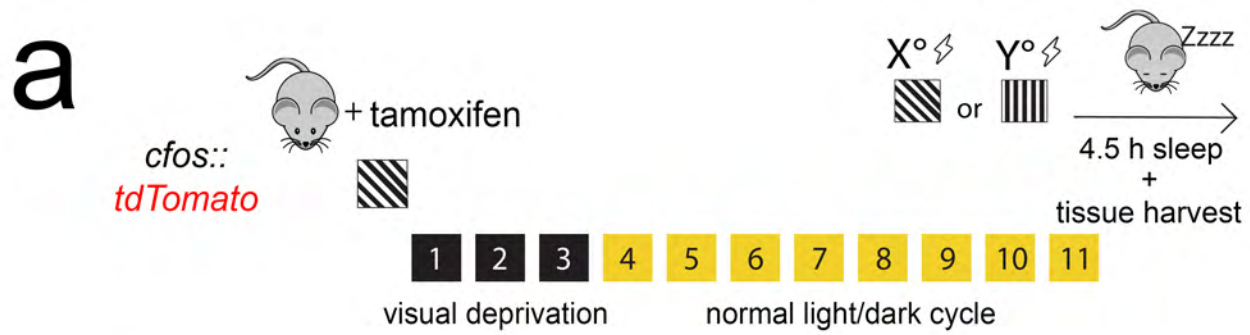
▨▨▨ alternate orientation

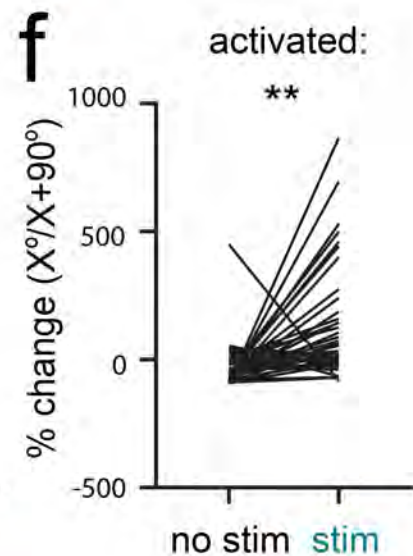
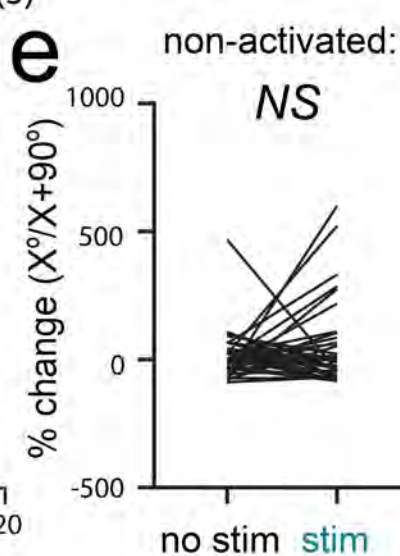
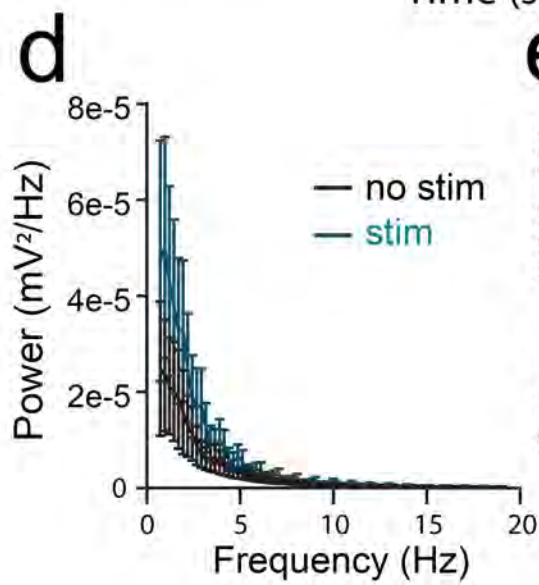
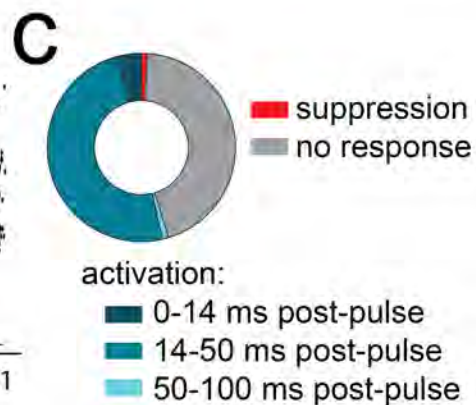
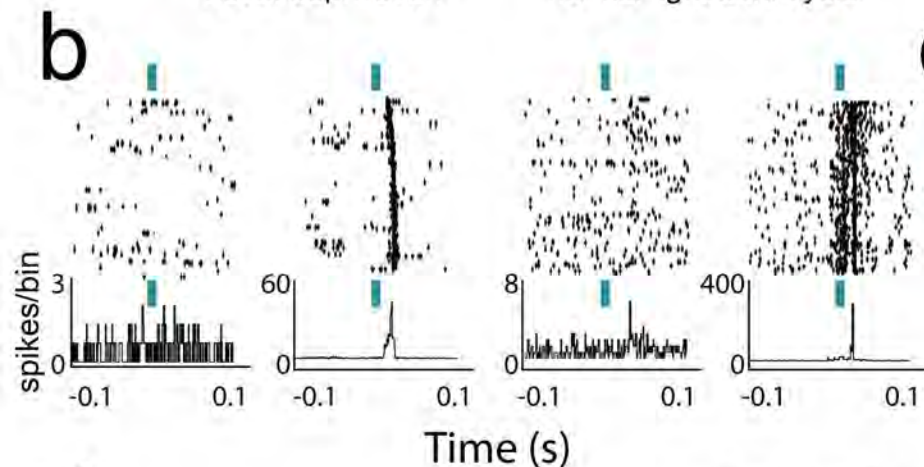
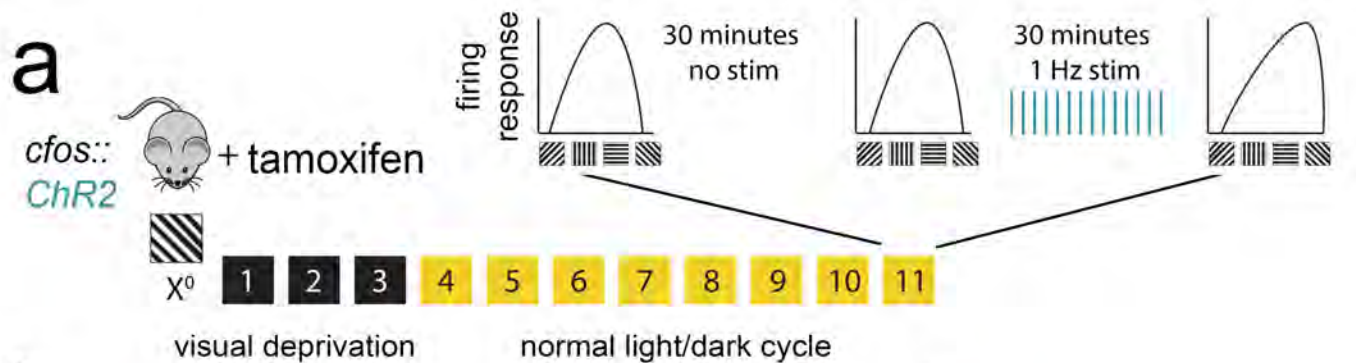


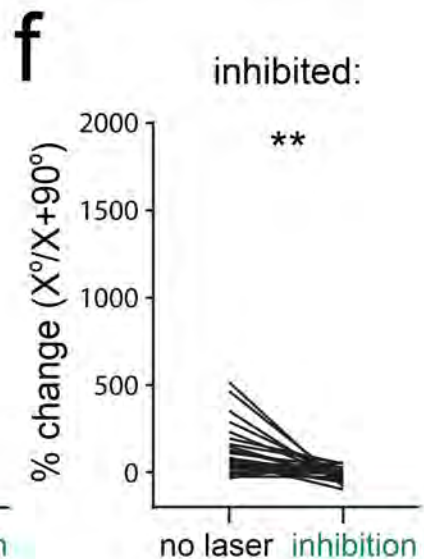
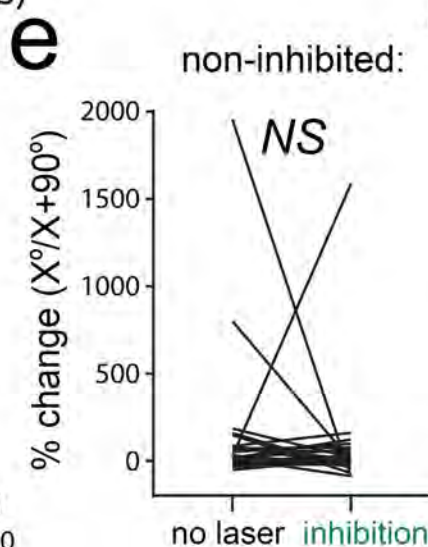
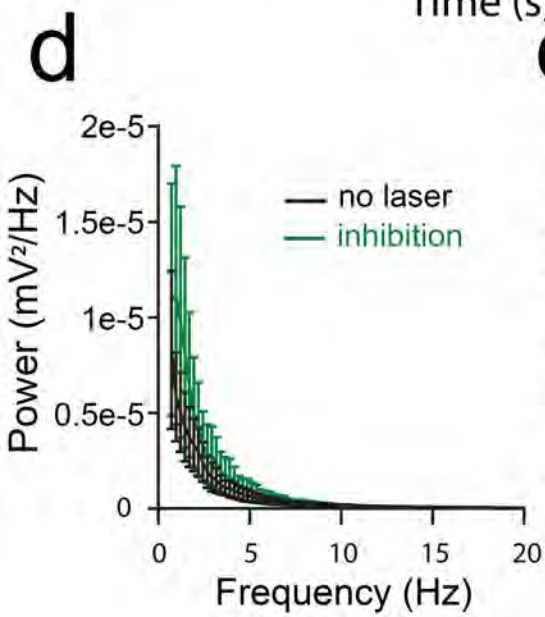
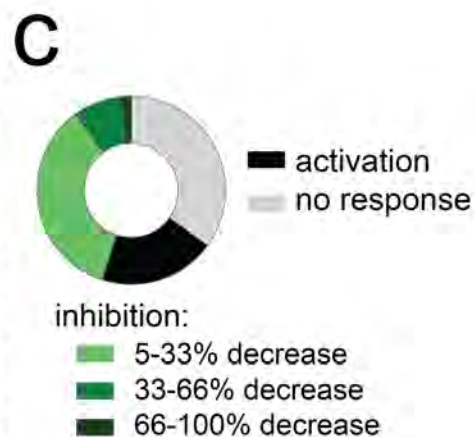
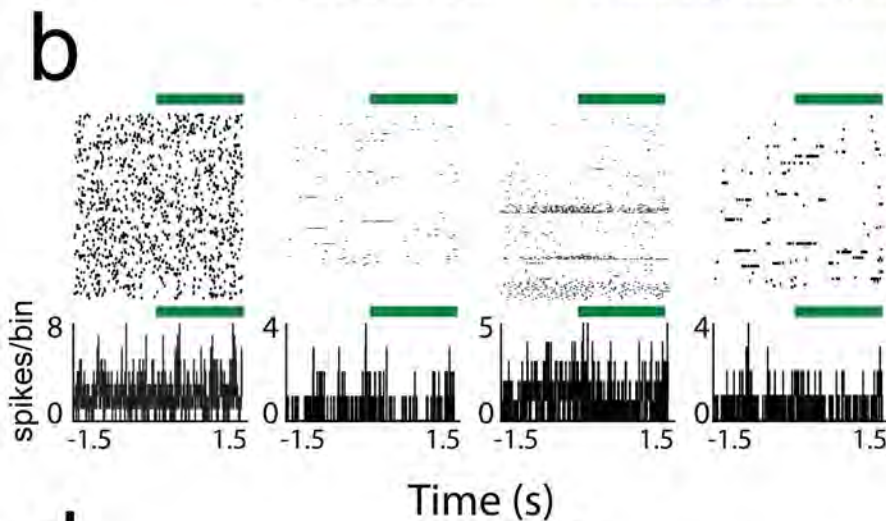
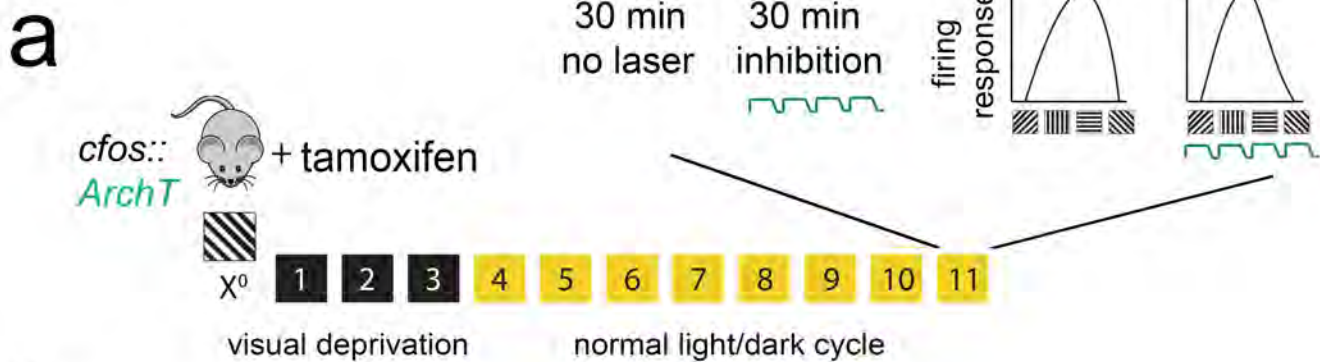
f

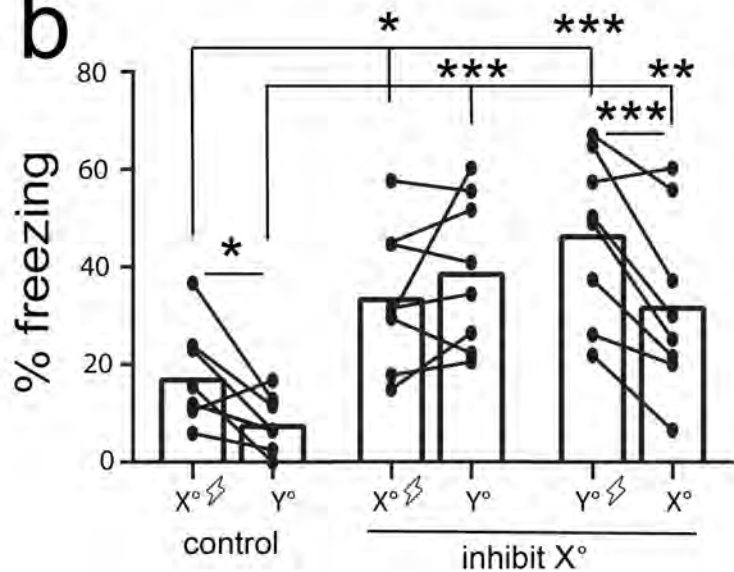
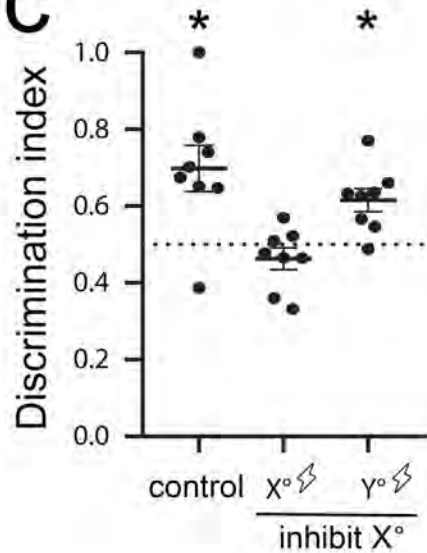


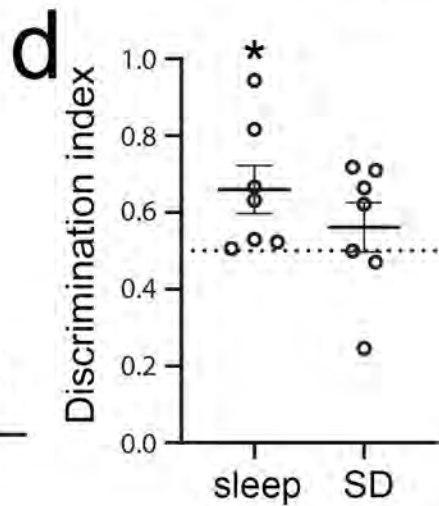
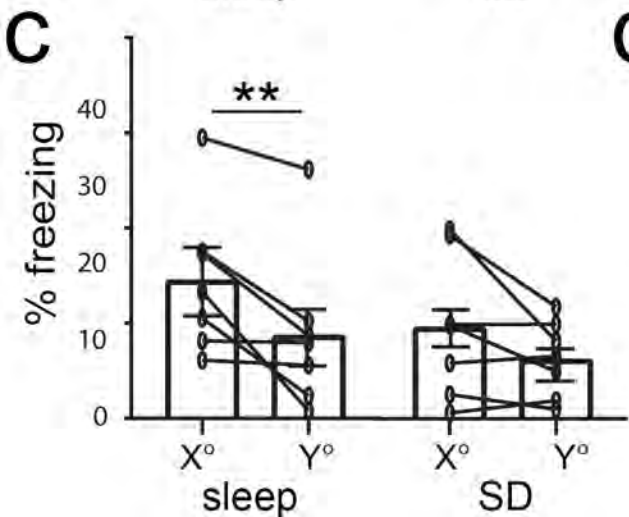
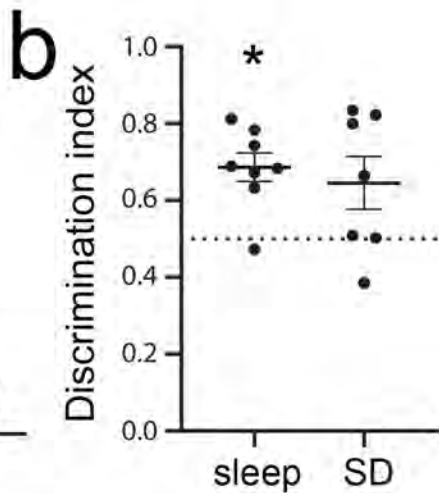
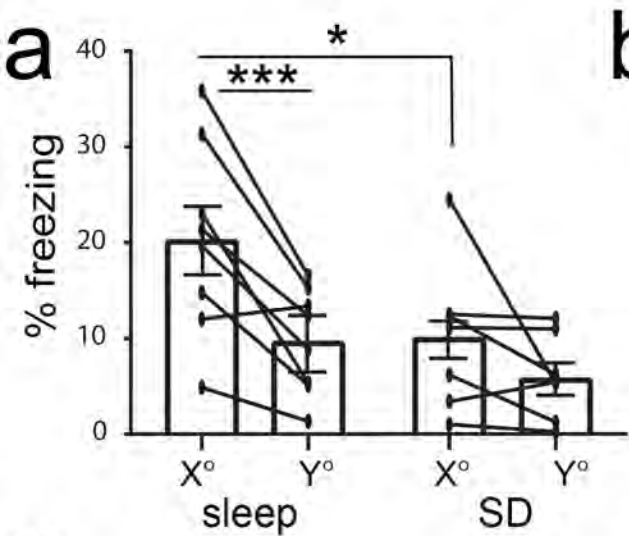




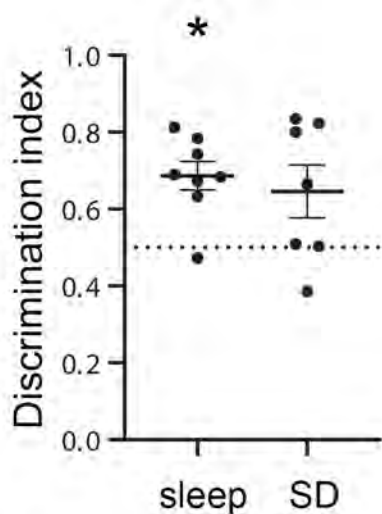
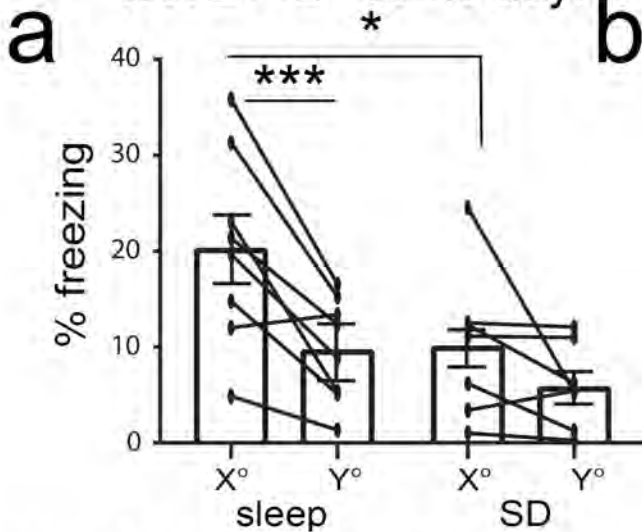




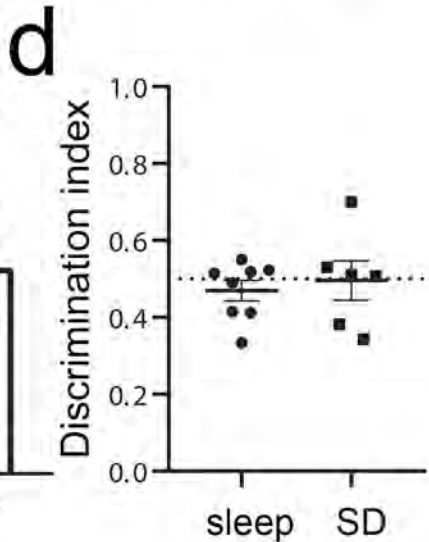
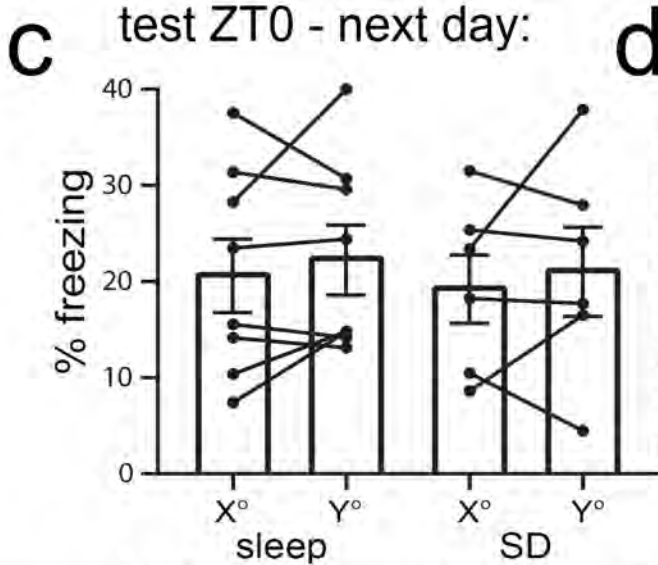
a**b****c**



test ZT12 - same day:



test ZT0 - next day:



test ZT12 - next day:

